Applied Radiation and Isotopes 226 (2025) 112063

Contents lists available at ScienceDirect

Applied Radiation and Isotopes

journal homepage: www.elsevier.com/locate/apradiso

Measurement of the ^{235}U fission cross section relative to the standard ^{10}B(n, α) reaction at the CERN n_TOF facility: Results for $E_n < 2$ eV

V. Michalopoulou [1,*], M. Diakaki [1], N. Kyritsis [1], M. Kokkoris [1], R. Vlastou [1], M. Mavromatakou-Karamitsiou [1], Z. Eleme [2], N. Patronis [2,3], O. Aberle [3], V. Alcayne [4], S. Amaducci [5], J. Andrzejewski [6], V. Babiano [7], M. Bacak [3], J. Balibrea-Correa [8], A.P. Bernardes [3], E. Berthoumieux [9], R. Beyer [10], M. Boromiza [11], D. Bosnar [12], M. Caamaño [13], F. Calviño [7], M. Calviani [3], D. Cano-Ott [4], A. Casanovas [7], D.M. Castelluccio [14,15], F. Cerutti [3], G. Cescutti [16,17], S. Chasapoglou [1], E. Chiaveri [3,18], G. Claps [19], P. Colombetti [20,21], N. Colonna [22], P. Console Camprini [15,14], G. Cortés [7], M.A. Cortés-Giraldo [23], L. Cosentino [5], S. Cristallo [24,25], S.F. Dellmann [26], M. Di Castro [3], M. Dietz [27], C. Domingo-Pardo [8], R. Dressler [28], E. Dupont [9], I. Durán [13], M. Eslami [29], S. Fargier [3], B. Fernández-Domínguez [13], P. Finocchiaro [5], V. Furman [30], A. Gandhi [11], F. García-Infantes [31,3], A. Gawlik-Ramięga [6], G. Gervino [20,21], S. Gilardoni [3], E. González-Romero [4], S. Goula [2], E. Griesmayer [32], C. Guerrero [23], F. Gunsing [9], C. Gustavino [33], J. Heyse [34], W. Hillman [18], D.G. Jenkins [29], E. Jericha [32], A. Junghans [10], Y. Kadi [3], K. Kaperoni [1], D. Koll [10], Y. Kopatch [30], M. Krtička [35], I. Ladarescu [8], C. Lederer-Woods [36], J. Lerendegui-Marco [8], G. Lerner [3], A. Manna [15,37], T. Martínez [4], A. Masi [3], C. Massimi [15,37], P. Mastinu [38], M. Mastromarco [22,39], E.A. Maugeri [28], A. Mazzone [22,40], E. Mendoza [4], A. Mengoni [14,15], P.M. Milazzo [16], R. Mucciola [20,41], E. Musacchio González [38], A. Musumarra [42,43], A. Negret [11], J.A. Pavón [23,3], M.G. Pellegriti [42], P. Pérez-Maroto [23], A. Pérez de Rada Fiol [4], J. Perkowski [6], C. Petrone [11], L. Piersanti [24,25], E. Pirovano [27], J. Plaza del Olmo [4], S. Pomp [44], I. Porras [31], J. Praena [31], J.M. Quesada [23], R. Reifarth [26], D. Rochman [28], Y. Romanets [45], A. Rooney [36], C. Rubbia [3], A. Sánchez-Caballero [4], M. Sabaté-Gilarte [3], D. Scarpa [38], P. Schillebeeckx [34], D. Schumann [28], A.G. Smith [18], N.V. Sosnin [36], M. Spelta [16,17], M.E. Stamati [2,3], G. Tagliente [22], A. Tamburrino [19], A. Tarifeño-Saldivia [8], D. Tarrío [44], P. Torres-Sánchez [31], S. Tosi [19], G. Tsiledakis [9], S. Valenta [35], P. Vaz [45], G. Vecchio [5], D. Vescovi [26], V. Vlachoudis [3], A. Wallner [10], C. Weiss [32], P.J. Woods [36], T. Wright [18], P. Žugec [12], the n_TOF collaboration[a]

[1] National Technical University of Athens, Greece
[2] University of Ioannina, Greece
[3] European Organization for Nuclear Research (CERN), Switzerland
[4] Centro de Investigaciones Energéticas Medioambientales y Tecnológicas (CIEMAT), Spain
[5] INFN Laboratori Nazionali del Sud, Catania, Italy
[6] University of Lodz, Poland
[7] Universitat Politècnica de Catalunya, Spain
[8] Instituto de Física Corpuscular, CSIC - Universidad de Valencia, Spain
[9] CEA Irfu, Université Paris-Saclay, F-91191 Gif-sur-Yvette, France
[10] Helmholtz-Zentrum Dresden-Rossendorf, Germany
[11] Horia Hulubei National Institute of Physics and Nuclear Engineering, Romania
[12] Department of Physics, Faculty of Science, University of Zagreb, Zagreb, Croatia
[13] University of Santiago de Compostela, Spain
[14] Agenzia nazionale per le nuove tecnologie, l'energia e lo sviluppo economico sostenibile (ENEA), Italy

* Corresponding author.
E-mail address: veatrikimich@mail.ntua.gr (V. Michalopoulou).
[a] www.cern.ch/ntof

https://doi.org/10.1016/j.apradiso.2025.112063
Received 3 March 2025; Received in revised form 19 July 2025; Accepted 21 July 2025
Available online 13 August 2025

[15] Istituto Nazionale di Fisica Nucleare, Sezione di Bologna, Italy
[16] Istituto Nazionale di Fisica Nucleare, Sezione di Trieste, Italy
[17] Department of Physics, University of Trieste, Italy
[18] University of Manchester, United Kingdom
[19] INFN Laboratori Nazionali di Frascati, Italy
[20] Istituto Nazionale di Fisica Nucleare, Sezione di Torino, Italy
[21] Department of Physics, University of Torino, Italy
[22] Istituto Nazionale di Fisica Nucleare, Sezione di Bari, Italy
[23] Universidad de Sevilla, Spain
[24] Istituto Nazionale di Fisica Nucleare, Sezione di Perugia, Italy
[25] Istituto Nazionale di Astrofisica - Osservatorio Astronomico d'Abruzzo, Italy
[26] Goethe University Frankfurt, Germany
[27] Physikalisch-Technische Bundesanstalt (PTB), Bundesallee 100, 38116 Braunschweig, Germany
[28] Paul Scherrer Institut (PSI), Villigen, Switzerland
[29] University of York, United Kingdom
[30] Affiliated with an institute covered by a cooperation agreement with CERN
[31] University of Granada, Spain
[32] TU Wien, Atominstitut, Stadionallee 2, 1020 Wien, Austria
[33] Istituto Nazionale di Fisica Nucleare, Sezione di Roma1, Roma, Italy
[34] European Commission, Joint Research Centre (JRC), Geel, Belgium
[35] Charles University, Prague, Czech Republic
[36] School of Physics and Astronomy, University of Edinburgh, United Kingdom
[37] Dipartimento di Fisica e Astronomia, Università di Bologna, Italy
[38] INFN Laboratori Nazionali di Legnaro, Italy
[39] Dipartimento Interateneo di Fisica, Università degli Studi di Bari, Italy
[40] Consiglio Nazionale delle Ricerche, Bari, Italy
[41] Dipartimento di Fisica e Geologia, Università di Perugia, Italy
[42] Istituto Nazionale di Fisica Nucleare, Sezione di Catania, Italy
[43] Department of Physics and Astronomy, University of Catania, Italy
[44] Department of Physics and Astronomy, Uppsala University, Box 516, 75120 Uppsala, Sweden
[45] Instituto Superior Técnico, Lisbon, Portugal

ARTICLE INFO

Keywords:
Fission
Micromegas
n_TOF
Cross-section

ABSTRACT

The neutron induced fission of ^{235}U is a very important reaction for nuclear technology applications and for the design of future systems to produce clean and safe energy. In addition, it is used as a reference reaction for neutron cross-section measurements, thus, its cross section is needed with a high accuracy over a wide energy range. In this work, the measurement for the ^{235}U(n,f) reaction was carried out at the n_TOF facility located at CERN, at experimental area EAR-2. The standard ^{10}B(n, α) reaction was used as reference, while a setup based on the gaseous Micromegas detectors was implemented for the detection of the fission fragments and α and ^{7}Li-particles of the two reactions, respectively. In order to determine the thickness of the ^{10}B sample NRA measurements were carried out at the National Center for Scientific Research "Demokritos".

1. Introduction

^{235}U is the most important isotope in nuclear applications and the only naturally occurring fissile nuclide. The neutron induced fission cross section of ^{235}U is widely used as a reference reaction in nuclear cross-section measurements over a wide energy region, nevertheless, it is only considered a standard at the thermal point, in the cross-section integral between 7.8 to 11 eV and between 150 keV to 200 MeV (Carlson et al., 2018). Experimental data of the n_TOF collaboration pointed out an overestimation of the evaluated neutron induced fission cross section of ^{235}U in the energy region 10 to 30 keV (Barbagallo et al., 2013), which is why a dedicated measurement was performed at the n_TOF collaboration to explore this issue (Amaducci et al., 2020), using a setup based on in-beam silicon detectors and implementing two standard reactions as references (^{6}Li(n,t) and ^{10}B(n, α)). The results of this work showed an overestimation in the evaluated libraries of the cross-section values between 9 and 18 keV by 5% (Amaducci et al., 2019). The analysis of the same experimental dataset in the energy region from 18 meV to 10 keV showed discrepancies between the experimental data and the evaluated libraries at few eV, in the energy region between 20 and 80 eV and in the region of 2 keV (Mastromarco et al., 2022).

Additional data for the ^{235}U(n,f) reaction using the standard ^{10}B(n, α) reaction as reference have become available from experimental areas EAR-1 and EAR-2 of the n_TOF facility, from the reference targets used in the measurement of the ^{243}Am(n,f), the data of the latter work being currently under analysis. The measurement was conducted using the gaseous Micromegas detectors, with the ^{10}B target being the first target incident to the neutron beam, followed by the ^{235}U one. Taking into account the importance of the ^{235}U(n,f) reaction, it was decided to analyze these data in order to extract the cross section and further assist future evaluations. The main advantages of this measurement is the almost 2π efficiency of the detector, rendering any correction for the efficiency of the setup negligible and the combination of the results from two experimental areas, will eventually reduce the systematic uncertainty of the results.

In this work, cross-section results from the experimental area EAR-2 for energies lower than 2 eV will be presented. The experimental procedure will be presented, in addition to NRA measurements in order to estimate the mass of the ^{10}B sample and its inhomogeneity, performed at the National Center for Scientific research N.C.S.R. "Demokritos" and extensive Monte Carlo simulations using the FLUKA code (Böhlen et al., 2014), in order to reproduce the experimental amplitude spectra of the targets. These simulations are the key for absolute cross-section results, since they introduce the main systematic uncertainty in the results.

2. Experimental setup

The experiment was performed at the neutron time-of-flight facility n_TOF at CERN (Barbagallo et al., 2013; Guerrero et al., 2013). At n_TOF the neutrons are produced via the spallation process of high energy protons impinging on a Pb target. A white neutron source is

produced from this interaction with energies ranging from thermal up to few hundred of MeVs. The neutrons arrive at three different experimental areas, namely EAR-1, EAR-2 and the recently commissioned NEAR station. Each area is located at a different distance from the spallation target, giving this way different characteristics to the neutron beam. EAR-1 is located 185 m horizontally from the spallation target, providing excellent neutron energy resolution. On the other hand, experimental area EAR-2 is located 19 m from the spallation target, having this way higher instantaneous neutron flux with the cost of neutron energy resolution, rendering however the area suitable for measurements of lower cross sections, lower mass samples and radioactive ones, since a better signal-to-noise ratio can be achieved there. The recently commissioned NEAR station is placed only 3 m from the center of the spallation target, providing this way much higher instantaneous neutron flux, with the goal to measure reactions that cannot be measured in the other to areas, because of the low cross section or the very low mass or both.

In the present work the experiment was performed at both experimental areas EAR-1 and EAR-2 with the use of Micromegas detectors, using the fission collimator with a diameter of 6 cm. The Micromegas detector is a gas detector consisting of three parts, the drift electrode, which is the target itself, the mesh electrode, which is a Cu plate with 35 μm holes on it and the anode electrode which is a Cu plate. The voltages applied in the three electrodes, create two electric field regions, one weak (≈1 kV/cm) located between the drift and the mesh electrode, the drift region, and one strong (≈50 kV/cm) located between the mesh and the anode electrode, the amplification region. Each detector is coupled with one sample, while all samples and detectors are placed in an aluminum chamber, filled with gas Ar:CF_4 (90:10) kept at constant pressure and room temperature, which is then placed in the neutron beam. This way all samples are measured simultaneously, under the same experimental conditions.

When a reaction occurs from the interaction of the neutron beam with the sample, two charged particles are created, namely a heavy and a light fission fragment in the case of the ^{235}U target and one α and one ^{7}Li nucleus in the case of the ^{10}B target, with one of two products of each reaction entering the detector gas, while the other escapes due to the kinematics. The charged particle creates secondary electrons as it moves along the drift region, which are drifted through the mesh holes guided from the electric field. The electrons are meeting there a much higher electric field and are creating additional electrons through avalanches. The signal, which is proportional to the energy deposited in the drift region, is collected from the mesh electrode.

The waveform of the signals is recorded through fast analog-to-digital converters and then analyzed in order to extract the amplitude and time-of-flight of each pulse, with the latter being converted to the energy of the neutron which caused each event.

2.1. Samples

The samples used for the measurements were produced at JRC-Geel (Sibbens et al., 2020). The boron sample was natural boron deposited on an Al backing consisting of 81.1% ^{11}B and 19.9% ^{10}B, which does not pose a problem in the measurements since no neutron-induced charged particle reaction is open below 7.2 MeV for ^{11}B, while the ^{235}U target had an enrichment of 99.934%. The diameter of both ^{235}U and ^{10}B samples was 6 cm, thus the samples being completely covered by the neutron beam.

The ^{235}U sample was characterized at the target preparation laboratory of JRC-Geel. The activity was determined by α-particle counting at a defined solid-angle (Pommé et al., 2003) and was found to be 9.80(5) Bq corresponding to a mass equal to 122.6(6) μg. The contribution from the ^{234}U, ^{236}U and ^{238}U decay was derived from the isotopic composition of the base material determined by mass spectrometry and the following mass ratios were found: $^{235}U/\mathrm{U}$ = 0.999336(7), $^{234}U/\mathrm{U}$ = 0.00035973(38), $^{236}U/\mathrm{U}$ = 0.00009629(27) and $^{238}U/\mathrm{U}$ = 0.000207(7), which have a negligible contribution in the counting spectrum of the ^{235}U(n,f) reaction. Additional information on the preparation and the characterization procedure can be found in Michalopoulou et al. (2023).

For the characterization of the boron target the Nuclear Reaction Analysis (NRA) technique was used. The mass of ^{11}B was estimated via the ^{11}B(p, α_0) reaction, while the ^{10}B mass was found according to the known isotopic ratio of the two isotopes in natural boron. More information on the NRA technique and the implemented differential cross sections can be found in Kokkoris et al. (2010).

The measurement was performed at the 5.5 MV Tandem accelerator of N.C.S.R. "Demokritos" in Athens, Greece. 2619 keV protons were guided to a goniometric chamber, where the boron target was placed. The energy of the proton beam was verified by the well-known 999.89 keV resonance of the ^{27}Al(p, γ) reaction, with the use of a HPGe detector for the detection of the 1779 keV γ-ray (1st excited state of the compound ^{28}Si nucleus). The produced α-particles were detected with the use of a Si surface barrier detector placed at 160° with respect to the proton beam. The current on the target did not exceed 200 nA throughout the measurement to avoid any possible thermal effects or degradation of the target. The program SIMNRA (Mayer, 1997) was used for the analysis of the experimental spectra, where the known differential cross-section data for the ^{11}B(p, α_0) reaction combined with evaluated stopping power data for protons and alphas from Ziegler–Biersack–Littmark (Ziegler et al., 1985) were used. The thickness of the boron target was adjusted in order to accurately reproduce the experimental spectrum. From the analysis the thickness of ^{10}B in the target was found 0.059 ±0.002 μg/cm^2. A typical experimental spectrum along with the simulated one are presented in Fig. 1, along with the peak identification. It can be seen that the alpha peak is slightly shifted in energy, due to the fact that the calibration of the detectors was done with protons. The pile-up has been taken into account in the simulations using the accurate model incorporated in the code (Mayer, 1997), however the triple pile-up which occurs between channels ≈595-750 is not taken into account by the simulations, which explains the difference between the experimental and the simulated spectra in this region. However, this does not pose a problem for the estimation of the target thickness, since no background from the triple pile-up is introduced under the ^{11}B(p, α_0)^{8}Be peak.

Since the counting rate of the ^{11}B(p, α_0) reaction did not allow for the lateral inhomogeneity study of the ^{11}B target, a thick ^{11}B target was used instead. This thick target was prepared at JRC-Geel with the same technique as the thin one and was also used in measurements at CERN. For the homogeneity tests, four different measurements were taken, equally distant from the geometrical center of the thick ^{11}B target and the lateral inhomogeneity did not exceed 5% in all cases, with respect to the central value.

3. Data analysis

The data analysis procedure aims at the recognition of the arrival time of each pulse, which is estimated relative to the γ-flash peak and the corresponding amplitude. The analysis is performed with a pulse shape analysis routine (PSA) (Žugec et al., 2016). A detailed description on the analysis procedure used in this type of experiments can be found in Michalopoulou et al. (2023). The experimental data are recorded in the so-called movies, where each movie corresponds to a different neutron bunch. The first peak in the movie is the γ-flash peak, which corresponds to a high energy deposition on the detector from γ-rays, high energy relativistic particles and high energy neutrons, all results from the spallation process. The time-of-flight of each pulse can be uniquely identified from the difference in the arrival time of each pulse from the γ-flash peak. The amplitude of each pulse can also be determined from the PSA. An amplitude spectrum for the ^{10}B target is shown in Fig. 2.

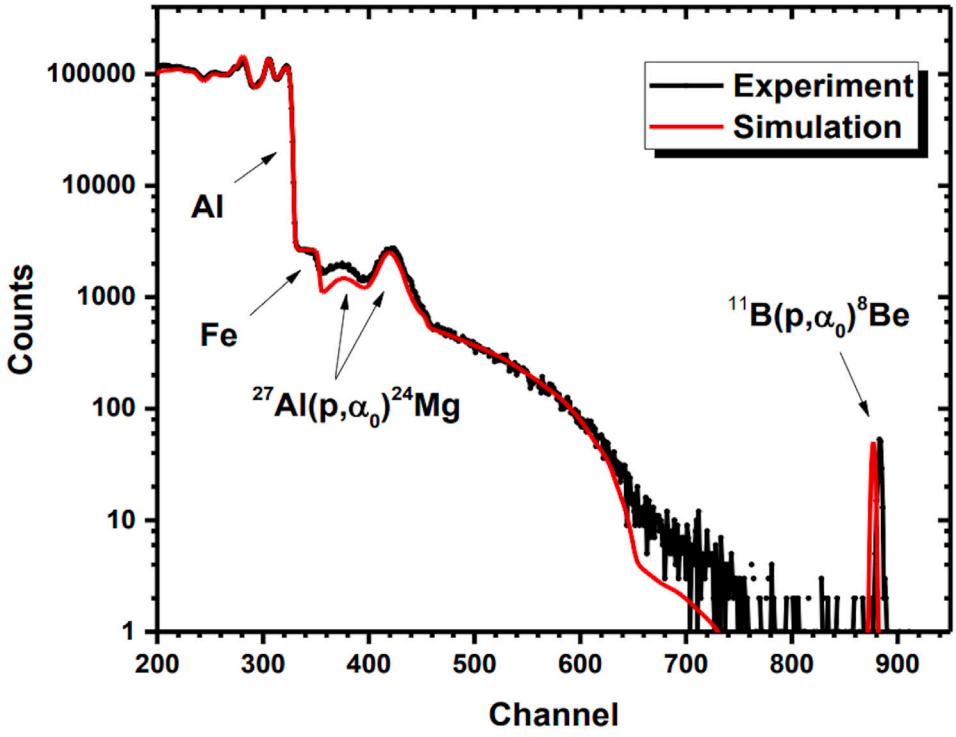

Fig. 1. Experimental spectrum taken at 160° for $E_{p,lab}$ = 2619 keV (black line) and the simulated spectrum with the SIMNRA code (red line). The $^{11}B(p, \alpha_0)$ is present in the spectrum, as well as the $^{27}Al(p, \alpha_0)$ from the backing of the target.

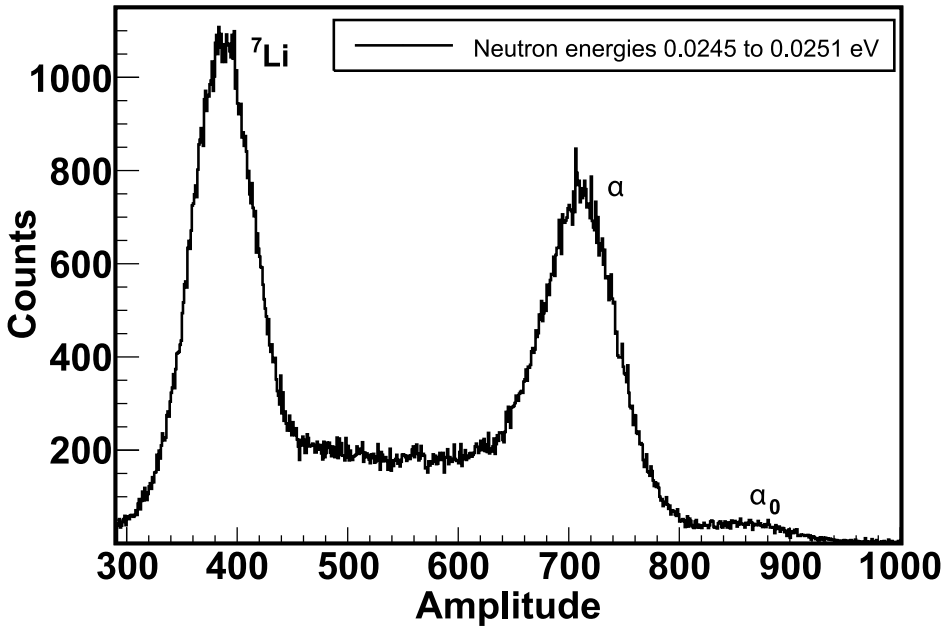

Fig. 2. Amplitude spectrum of the ^{10}B target for energies between 0.0245 to 0.0251 eV, from experimental area EAR-2.

3.1. FLUKA simulations

The energy deposition in the Micromegas detector was studied via Monte-Carlo simulations performed with the FLUKA code (Böhlen et al., 2014), in order to reproduce the experimental amplitude spectra via the simulations. This is an important part of this work, in order to deduce absolute cross-section values for the $^{235}U(n,f)$ reaction, which can be compared to values normalized in the thermal point and in the integral between 7.8 to 11 eV, minimizing this way the systematic uncertainty of the final results. The simulations are necessary to estimate the amplitude cut correction, which is introduced in the analysis in order to exclude noise in the lower channels, plus α-particles from the radioactivity of the targets in the case of ^{235}U.

In the simulations the energy deposition in the Micromegas drift gap was estimated for the ^{10}B and ^{235}U targets respectively, since the signal of each event is proportional to the energy deposition of the charged particle (α, ^{7}Li or fission fragment) in the drift region. In the case of the ^{235}U target the kinetic energy, atomic mass and mass number of the fission fragments were generated via the GEF code (Schmidt et al., 2016), while an isotropic emission of the fission fragments was

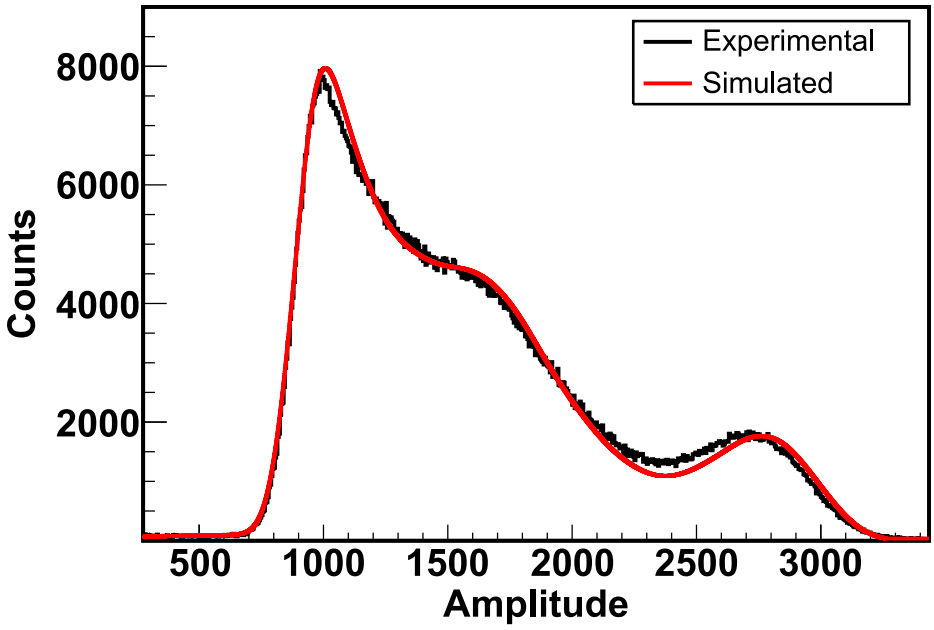

Fig. 3. Simulated energy deposition of fission fragments for the ^{235}U target (red line), compared with the experimental one from experimental area EAR-2 (black line).

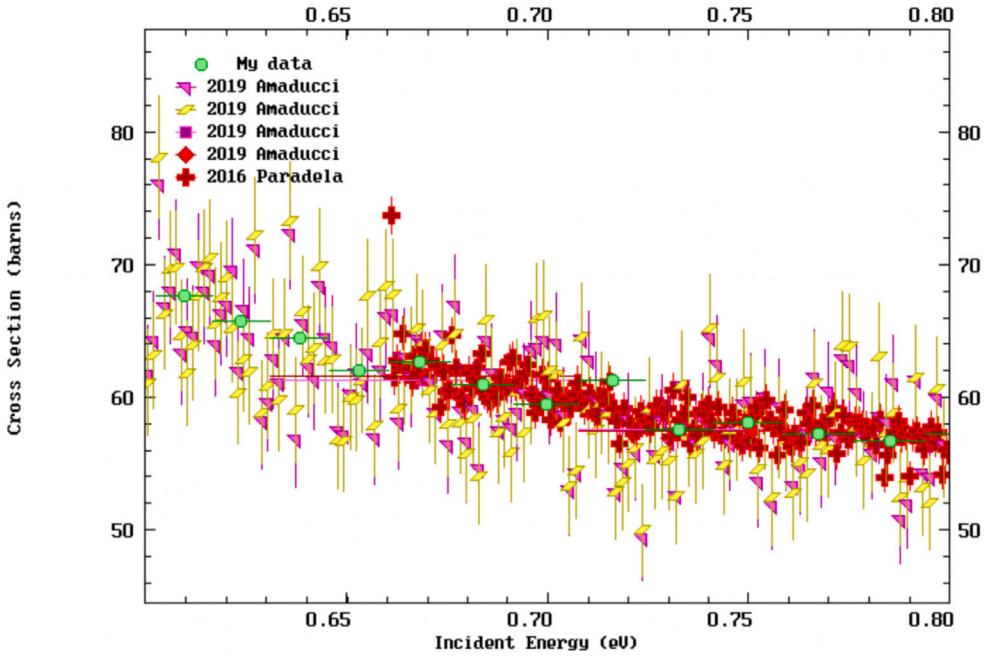

Fig. 4. Cross-section of the ^{235}U(n,f) reaction from the EAR-2 measurement, estimated using standard ^{10}B(n, α) reaction as reference in the energy region 0.6 to 0.8 eV in 100 bpd, along with the latest experimental data available in EXFOR and the evaluated libraries ENDF/B-VIII.1 and JEFF-3.3.

assumed. A more detailed description on how the simulations were performed in the case of the ^{235}U target is presented in Michalopoulou et al. (2023). In the case of the ^{10}B sample a mono-energetic neutron beam can be used as the primary beam or the charged products of the reaction can be simulated by a user-defined source routine, with the energies expected from the kinematics of the reaction, while no angular distribution is assumed.

The simulated spectra are calibrated from energy to channels and then convoluted with a skewed gaussian function in order to reproduce the experimental ones. The comparison between the experimental and simulated spectra from the experimental area EAR-2 data for the ^{235}U target is shown in Fig. 3.

3.2. Estimation of neutron energy

An important part of the data analysis is the conversion of the neutron time-of-flight, corresponding to a specific event detected, into the neutron energy. The time-of-flight is estimated relative to the γ-flash peak during the pulse shape analysis. This conversion is crucial for two reasons: first, the counts recorded in a given time-of-flight interval must be accurately converted to the correct energy; second, because this study involves a relative measurement, the cross-section of the standard ^{10}B(n, α) reaction – evaluated at the correct energy – must be considered in order to estimate the neutron flux. However, after their production, neutrons travel a certain distance within the spallation target, known as the moderation length. This moderation

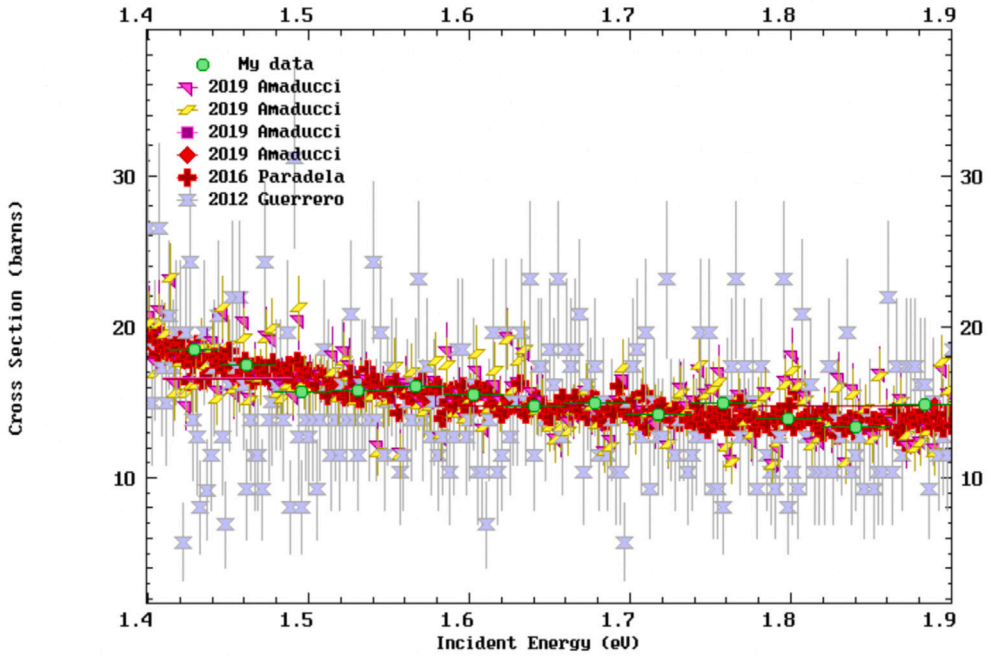

Fig. 5. Cross-section of the ^{235}U(n,f) reaction from the EAR-2 measurement, estimated using standard ^{10}B(n, α) reaction as reference in the energy region 1.4 to 1.9 eV in 100 bpd, along with the latest experimental data available in EXFOR and the evaluated libraries ENDF/B-VIII.1 and JEFF-3.3.

length is not a fixed value but rather a distribution that depends on the neutron energy. To accurately convert the neutron time-of-flight to energy, the following methodology was applied in this work: the time-of-flight spectrum from the ^{235}U targets was matched to the resonance energies known from the ENDF/B-VIII.1 (Brown et al., 2018) library. From this match, an equivalent constant flight path was determined, optimized to reproduce the resonance energies in the 1 to 100 eV range, with an accuracy better than 1% at all resonance points. Using this equivalent flight path, the corresponding flight path length for the boron sample was then calculated based on the known geometrical distance between the two targets inside the chamber. Nevertheless, to precisely analyze the resonances, the facility's resolution function must also be taken into account through a resonance analysis code, which is planned for future work.

4. Results and discussion

The results for the ^{235}U(n,f) cross section from the experimental area EAR-2 measurement using the standard ^{10}B(n, α) reaction as reference are presented in Figs. 4 and 5, normalized to the standard integral cross section between 7.8 and 11 eV using 100 bins per decade (bpd). Two energy regions are presented in this work, from 0.6 to 0.8 eV and from 1.4 to 1.9 eV, where no resonances are present. Additional analysis with a resonance analysis code, such as SAMMY (Larson, 2008), taking into account the response function of experimental area EAR-2 is required in order to extract information of the resonances and the regions close to them. This work will be carried out in the future. The results are presented along with only the latest available experimental data in EXFOR (Otuka et al., 2014), namely the data of Amaducci et al. (2019), Paradela et al. (2016) and Guerrero et al. (2012) and the evaluated libraries ENDF/B-VIII.1 (Brown et al., 2018) and JEFF-3.3 (Plompen et al., 2020).

As seen in the figures, the results of this work are in very good agreement with the ENDF/B-VIII.1 library in the energy region 0.6 to 0.8 eV, while the JEFF-3.3 evaluation is slightly higher than ENDF/B-VIII.1 and the present work. In the energy range 1.4 and 1.9 eV, the data of this work are in better agreement with the ENDF/B-VIII.1 library up to ≈1.55 eV, while at higher energies the data are in better agreement with the JEFF-3.3 library.

It is observed in these two energy regions that discrepancies exist on the latest evaluated libraries of the well known reaction ^{235}U(n,f), highlighting the need for measurements in order to improve the evaluations and make it possible to extend the energy region where it is considered a standard.

With the use of a resonant analysis code, the ^{235}U(n,f) reaction can be studied in the region of the resonances, providing new data there. Lastly, the comparison between the experimental data from experimental areas EAR-1 and EAR-2 will also minimize systematic uncertainties.

CRediT authorship contribution statement

V. Michalopoulou: Writing – review & editing, Writing – original draft, Supervision, Methodology, Investigation. **M. Diakaki:** Writing – review & editing, Supervision, Funding acquisition. **N. Kyritsis:** Data curation. **M. Kokkoris:** Writing – review & editing, Methodology. **R. Vlastou:** Writing – review & editing, Supervision. **M. Mavromatakou-Karamitsiou:** Formal analysis, Data curation. **Z. Eleme:** Data curation. **N. Patronis:** Supervision, Data curation. **n_TOF collaboration:** Data curation.

Declaration of competing interest

The authors declare the following financial interests/personal relationships which may be considered as potential competing interests: Veatriki Michalopoulou reports financial support was provided by Hellenic Foundation for Research and Innovation. Maria Diakaki reports financial support was provided by Hellenic Foundation for Research and Innovation. Veatriki Michalopoulou reports travel was provided by Euratom Research and Training Programme. Author Veatriki Michalopoulou has rev If there are other authors, they declare that they have no known competing financial interests or personal relationships that could have appeared to influence the work reported in this paper.

Acknowledgments

This project is carried out within the framework of the National Recovery and Resilience Plan Greece 2.0, funded by the European Union–NextGenerationEU (Implementation body: HFRI)

This project has received funding from the Euratom research and training programme 2014–2018 under grant agreement No 847594 (ARIEL).

Data availability

Data will be made available on request.

References

Amaducci, S., et al., 2019. Measurement of the ^{235}U(n, f) cross section relative to the ^{6}Li(n, t) and ^{10}B(n, α) standards from thermal to 170 kev neutron energy range at n_TOF. Eur. Phys. J. A 55, 120. http://dx.doi.org/10.1051/epjconf/202023908002.

Amaducci, S., et al., 2020. Accurate measurement of the standard ^{235}U(n, f) cross section from thermal to 170 kev neutron energy. EPJ Web Conf. 239, 08002. http://dx.doi.org/10.1051/epjconf/202023908002.

Barbagallo, M., et al., 2013. High-accuracy determination of the neutron flux at n_TOF. Eur. Phys. J. A 49, 156. http://dx.doi.org/10.1140/epja/i2013-13156-x.

Böhlen, T.T., et al., 2014. The FLUKA code: Developments and challenges for high energy and medical applications. Nucl. Data Sheets 120, 211214. http://dx.doi.org/10.1016/j.nds.2014.07.049.

Brown, D.A., et al., 2018. ENDF/B-VIII.0: the 8th major release of the nuclear reaction data library with CIELO-project cross sections, new standards and thermal scattering data. Nucl. Data Sheets 148, 1. http://dx.doi.org/10.1016/j.nds.2018.02.001.

Carlson, A.D., et al., 2018. Evaluation of the neutron data standards. Nucl. Data Sheets 148, 143–188. http://dx.doi.org/10.1016/j.nds.2018.02.002.

Guerrero, C., et al., 2012. Simultaneous measurement of neutron-induced capture and fission reactions at CERN. Nucl. Eur. Phys. J. A 48, 29. http://dx.doi.org/10.1140/epja/i2012-12029-2.

Guerrero, C., et al., 2013. Performance of the neutron time-of-flight facility n_TOF at CERN. Nucl. Eur. Phys. J. A 49, 1. http://dx.doi.org/10.1140/epja/i2013-13027-6.

Kokkoris, M., et al., 2010. Differential cross sections for the ^{11}b(p, α_0)^{8}be and ^{11}b(p, p_0)^{11}b reactions, suitable for ion beam analysis. Nucl. Instrum. Methods Phys. Res. B 268, 3539–3545. http://dx.doi.org/10.1016/j.nimb.2010.09.013.

Larson, N.M., 2008. Updated users' guide for SAMMY: Multilevel R-matrix fits to neutron data using Bayes' equations, ORNL/TM-9179/R8 ENDF-364/R2.

Mastromarco, M., et al., 2022. High accuracy, high resolution ^{235}U(n, f) cross section from n_TOF (CERN) from 18 meV to 10 keV. Eur. Phys. J. A 58, 147. http://dx.doi.org/10.1051/epjconf/202023908002.

Mayer, M., 1997. SIMNRA User's Guide, Report IPP 9/113. Max–Planck-Institut für Plasmaphysik, Garching, Germany.

Michalopoulou, V., et al., 2023. Measurement of the neutron-induced fission cross section of ^{230}Th at the CERN n_TOF facility. Phys. Rev. C 108, 014616. http://dx.doi.org/10.1103/PhysRevC.108.014616.

Otuka, N., et al., International Collaboration, 2014. Towards a more complete and accurate experimental nuclear reaction data library (EXFOR): Between nuclear reaction data centres (NRDC). Nucl. Data Sheets 120, 272–276. http://dx.doi.org/10.1016/j.nds.2014.07.065.

Paradela, C., et al., 2016. High accuracy ^{235}U(n, f) data in the resonance energy region. EPJ Web Conf. 111, 02003. http://dx.doi.org/10.1051/epjconf/201611102003.

Plompen, A.J.M., et al., 2020. The joint evaluated fission and fusion nuclear data library, JEFF-3.3. Eur. Phys. J. A 56, 181. http://dx.doi.org/10.1140/epja/s10050-020-00141-9.

Pommé, S., et al., 2003. An algorithm for the solid angle calculation applied in alpha-particle counting. Nucl. Instrum. Meth. A 505, 286. http://dx.doi.org/10.1016/S0168-9002(03)01070-2.

Schmidt, K.-H., et al., 2016. General description of fission observables: GEF model code. Nucl. Data Sheets 131, 107–221. http://dx.doi.org/10.1016/j.nds.2015.12.009.

Sibbens, G., et al., 2020. Target preparation for neutron-induced reaction experiments. EPJ Web Conf 229 (04003), http://dx.doi.org/10.1051/epjconf/202022904003.

Ziegler, J.F., Biersack, J.P., Littmark, U., 1985. The Stopping and Range of Ions in Solids. Pergamon Press, New York.

Žugec, P., et al., 2016. Pulse processing routines for neutron time-of-flight data. Nucl. Instrum. Meth. A 812 (134), http://dx.doi.org/10.1016/j.nima.2015.12.054.